Incident indicators for freeway traffic flow models

Communications in Transportation Research 2 (2022) 100060

Contents lists available at ScienceDirect

Communications in Transportation Research

journal homepage: www.journals.elsevier.com/communications-in-transportation-research

Full Length Article

Incident indicators for freeway traffic flow models

Azita Dabiri [a], Balázs Kulcsár [b,*]

[a] Delft Center for Systems and Control, Delft University of Technology, 2628 CN, Delft, the Netherlands
[b] Department of Electrical Engineering, Chalmers University of Technology, 41296, Gothenburg, Sweden

ARTICLE INFO

Keywords:
Macroscopic traffic flow models
Aw-Rascle model
Traffic accidents
Moving horizon
PDE
ODE
Multi stage numerical scheme

ABSTRACT

Developed in this paper is a traffic flow model parametrised to describe abnormal traffic behaviour. In large traffic networks, the immediate detection and categorisation of traffic incidents/accidents is of capital importance to avoid breakdowns, further accidents. First, this claims for traffic flow models capable to capture abnormal traffic condition like accidents. Second, by means of proper real-time estimation technique, observing accident related parameters, one may even categorize the severity of accidents. Hence, in this paper, we suggest to modify the nominal Aw-Rascle (AR) traffic model by a proper incident related parametrisation. The proposed Incident Traffic Flow (ITF) model is defined by introducing the incident parameters modifying the anticipation and the dynamic speed relaxation terms in the speed equation of the AR model. These modifications are proven to have physical meaning. Furthermore, the characteristic properties of the ITF model is discussed in the paper. A multi stage numerical scheme is suggested to discretise in space and time the resulting non-homogeneous system of PDEs. The resulting systems of ODE is then combined with receding horizon estimation methods to reconstruct the incident parameters. Finally, the viability of the suggested incident parametrisation is validated in a simulation environment.

1. Introduction

The unpredictable nature of human behavior as well as the temporal changes in the road geometry due to the constructions, accidents or weather conditions can bring unexpected changes in the traffic systems' dynamics. Although the current traffic flow models have been successfully used in various model-based traffic estimation and control problems such as Luspay et al. (2011); Dabiri et al. (2017); Dabiri and Kulcsár (2017); Hajiahmadi et al. (2016); Hegyi et al. (2005b,2005a, 2006), in the presence of the abnormal conditions, these models are not adequate for model-based traffic management. These nominal models are not able to capture the changes in the dynamics of the traffic when, e.g., an accident happens in the road or when the drivers are experiencing hard weather condition or fog.

With such motivation, some researches have been conducted in the past years to investigate how to properly model the abnormality in the traffic situation caused by an incident. The main idea in these research is to modify the nominal traffic model METANET Cremer and Papageorgiou (1981) such that the modified model be able to take the incident effect into account. Along this line, Sanwal et al. (1996) has proposed to model the accident as a lane drop and add a modification term in the speed equation of the METANET model to reflect the effect of an accident on the traffic mean speed. However, this modified model neglects the fact that naturally, drivers may change their driving behaviour in the presence of an accident. By means of analysing real traffic incidents, it has been found in Knoop et al. (2009) and Knoop (2009) that distribution of drivers reaction time increases at incident locations. In Wang et al. (2009), an Extended Kalman Filter is used to estimate abrupt changes in the core model parameters of the equilibrium speed due to an incident. By means of the online monitoring of these parameters, it was possible to capture the effect of incidents on the real sites. As a consequence, due to changing equilibrium speed profile, the relaxation term is modified, i.e. whenever incident happens, the average drivers relax their speed differently. In Dabiri and Kulcsár (2015), a bi-parameter approach is provided in order to separate drivers' behaviour and road geometry related effects of incidents within the framework of discretised Payne-Whitham (PW) second order traffic flow models.

The PW model suffers from few drawbacks Daganzo (1995): 1) The anisotropy condition is not preserved in the PW model. More specifically, vehicles in PW model could be effected by the stimuli from behind. This is due to the fact that one of the characteristic speed of the resulting hyperbolic system is higher than the traffic mean speed itself. This

* Corresponding author.
E-mail addresses: a.dabiri@tudelf.nl (A. Dabiri), kulcsar@chalmers.se (B. Kulcsár).

https://doi.org/10.1016/j.commtr.2022.100060
Received 26 January 2022; Received in revised form 29 March 2022; Accepted 29 March 2022
Available online xxxx

implies the unrealistic situation in which information travel faster than the vehicles. 2) PW model may generate negative speed in some conditions where the spacial derivative of the density is large. These drawbacks were addressed in the AR model developed by Aw and Rascle in Aw and Rascle (2000). The Aw-Rascle-Zhang (ARZ) model which belongs to the family of AR model is an alternative to the PW model which was criticised by Daganzo in Daganzo (1995) for the mentioned inadequacy. Within the similar line of thought as in Dabiri and Kulcsár (2015), in this paper, we aim at parametrising the ARZ macroscopic traffic flow model. This model is parametrised in this paper to generate the corresponding Incident Traffic Flow (ITF) model. This parametrisation will introduce some degree of freedom for modeling the abnormal traffic conditions. Within this macroscopic framework, we also aim at analysing these parameters. The suggested methodology consists (i) of using dynamic relaxation of traffic speed with time and space dependent incident parameter and (ii) of modifying the anticipation term in the speed equation of the AR model. We also show that the ITF model suggested in this paper inherits the same favourable properties of the nominal AR model. Moreover, analysis and discretisation of the proposed continuous-time macroscopic model is accompanied with proposing an online incident parameter estimation routine (nonlinear and constrained receding horizon estimation). A microscopic traffic simulator is used to show the viability of traffic incident reconstruction by online monitoring the incident parameter of the macroscopic ITF model.

The paper is organized as follows: first by defining incident related parameters, the incident traffic flow model (ITF) is defined and explained in the next section. It follows by a discussion on the mathematical properties of the model, its characteristics and bounds for the incident parameters in Section 3. In order to discretise the ITF model, Godunov scheme with splitting method is used in Section 4. An incident parameter estimation method is presented in Section 5. In Section 6, the proposed ITF model is validated using a simulation dataset for a hypothetical incident corrupted freeway. Remarks and future works are concluded in Section 7.

2. Incident affected Aw-Rascle-Zhang model

We build the incident traffic flow (ITF) model suggested in this paper upon the nominal Aw-Rascle-Zhang (ARZ) model. The ARZ model is a macroscopic traffic flow model which is used to describe the average traffic behaviour in normal condition. But as we see in the sequel, the ARZ model is unable to capture the traffic dynamics in abnormal conditions like accident. To fill the gap, the extension of the ARZ model which we call the ITF model is proposed in this section.

2.1. Aw-Rascle-Zhang model

Let us start with the description of the Aw-Rascle (AR) model presented in Rascle (2002) and get a general overview on the properties of this model. Based on the AR model, traffic dynamics can be described by use of two partial differential equations, namely conservation and momentum equations as

$$\rho_t + (\rho v)_x = 0, \tag{1}$$

$$\phi \quad = (v + P(\rho))_t + v(v + P(\rho))_x = \frac{V_e(\rho) - v}{\tau} \quad . \tag{2}$$

where ρ and v are the density and the mean speed and subscripts $(\cdot)_t$ and $(\cdot)_x$ account for the partial derivatives with respect to time and space respectively. $P(\rho)$, which is a non-decreasing function of the density, stands for the pressure term in analogy to gas dynamics. The relaxation term in the right hand side of Eq. (2) with $V_e(\rho)$ is the equilibrium speed. Equilibrium speed which is a function of density stands for a speed value that according to the traffic conditions, drivers may feel safe to choose. In this paper, taken from Mammar et al. (2009), the following equilibrium speed–density relationship is chosen:

$$V_e(\rho) = \begin{cases} V_{\max} - \dfrac{\rho}{\rho_{cr}}(V_{\max} - V_{cr}) & \text{case 1} \\ \dfrac{1}{\rho}\left(W_{\max}(\rho_{\max} - \rho_{cr}) + \varphi(\rho_{\max} - \rho)^2\right) & \text{case 2} \end{cases}$$

$$\varphi = \frac{Q_{\max}}{(\rho_{\max} - \rho_{cr})^2} - \frac{W_{\max}}{(\rho_{\max} - \rho_{cr})}, \tag{3}$$

with $W_{\max}$ as the model parameter and $V_{\max}$ and $\rho_{\max}$ are the free speed and jam density, respectively. If ρ_{cr} stands for the density in which the traffic flow is maximum, case 1 in the equilibrium speed description happens when $0 \le \rho \le \rho_{crit}$ while case 2 is valid if $\rho_{crit} \le \rho \le \rho_{\max}$.

To describe the pressure term $P(\rho)$ introduced in the AR model, let us rewrite the momentum Eq. (2) as

$$v_t + \left(v - \rho(P(\rho))_\rho\right)v_x = \frac{V_e(\rho) - v}{\tau}, \tag{4}$$

where $(\cdot)_\rho$ accounts for the partial derivative with respect to ρ. This representation is consistent with the following momentum equation suggested in Zhang (2002):

$$v_t + \left(v + \rho(V_e(\rho))_\rho\right)v_x = \frac{V_e(\rho) - v}{\tau}. \tag{5}$$

The representations Eqs. (4) and (5) are equivalent with Mammar et al. (2009) if the traffic pressure term be defined as

$$P(\rho) = V_{\max} - V_e(\rho). \tag{6}$$

Substituting Eq. (6) in Eq. (2) results in a reformulation of the AR model which is known in the literature as the Aw-Rascle-Zhang (ARZ) model. As seen in Eq. (6), the pressure term in the ARZ is defined as function of speed; the difference between the maximum speed that drivers can take and the equilibrium speed. In other words, traffic pressure is the amount of speed offset that drivers should have from the maximum speed due to the interaction with other vehicles in the road. The more intense this interaction, the larger the pressure term.

By defining $U = (\rho, v)$, it is easy to see that Eq. (1) along with Eq. (4) can be formulated as:

$$U_t + A(U)U_x = S(U). \tag{7}$$

It is known that the eigenvalues of $A(U)$ called characteristic speed determine how the traffic disturbance propagates in a traffic stream. It is easy to verify that the characteristic speed of (7) are equal to

$$\lambda_1 = v - \rho P_\rho \le \lambda_2 = v. \tag{8}$$

Since both of the eigenvalues are less or equal than the traffic speed, we can conclude that the anisotropic property of the traffic flow is respected in the ARZ model. This means that the propagation speed of the information can not be higher than traffic speed itself. In other words, drivers are not influenced by the traffic condition behind them Rascle (2002). This property is counted as one of the strength point of the AR (and ARZ) model compared to PW Daganzo (1995).

Having introduced the ARZ model, we are now ready to use this description for traffic incident parametrisation. It should be emphasized that incident is a general term we use to refer to any abnormal traffic condition. Hence, the focus of this paper is not only on the accidents but also on any possible reason (e.g., unusual harsh weather condition or rubbernecking) which may diverge the traffic behaviour from its normal.

2.2. Incident traffic flow (ITF) model

To have a better understanding of the change that an incident may cause in the traffic behaviour, let us start with the following example.

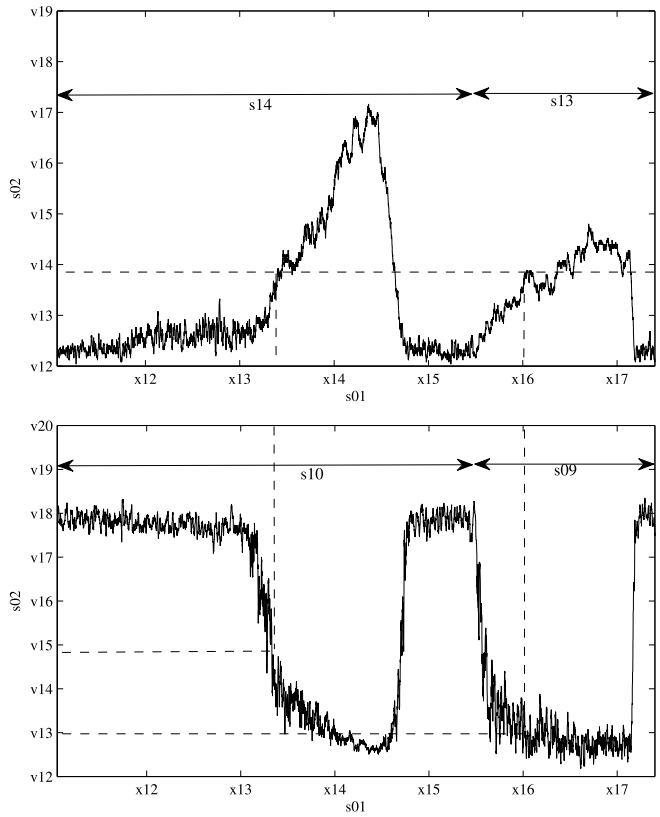

Fig. 1. Density and speed variation in segment i. At $t = 90$ min, incident happens in segment $i + 1$.

Example 1. Using the simulation environment, speed and density profile of an incident free traffic flow in a freeway segment i is compared with the incident affected flow and the results are depicted in Fig. 1. In this scenario, two different types of congestion are created; the first one which occurs at $t = 40$ min and due to the increased demand volume and the second one at $t = 90$ min and due to the occurrence of a traffic incident in the upstream segment $i + 1$ (see the case study in Section 6 for further details). It is observed from Fig. 1 that around a selected density, mean speed in incident-corrupted data can be significantly lower than the corresponding incident-free average speed. Moreover, the maximum flow under traffic incident can be reached at a relatively low density.

In line with the above observations, a generic method in this section is proposed to extend the nominal ARZ model in order to capture the effect of an incident in the traffic behaviour. Our intention is to relate the traffic incident to the traffic pressure term in the ARZ models, i.e., instead of recursively identifying changes in the equilibrium speed $V_e(\rho)$ as suggested in Wang et al. (2009), we propose to shape it through an incident parameter.

As explained in Section 2, the pressure term $P(\rho)$ describes the mean speed reduction due to the interaction among cars. Whenever an incident occurs, drivers may differently react to it compared to regular traffic condition. Drivers may reduce their speed faster and sooner to feel safe, to be more vigilant and/or to select their headways more carefully Knoop et al. (2009); Knoop (2009). We describe theses differences in the drivers' interaction by appropriately parametrising the traffic pressure term. We therefore introduce an incident parameter called α^*(s) resulting in a modified incident pressure term $P^*(\rho)$ as

$$P^*(\rho) = V_{\max} - \left(1 + \frac{\alpha^*}{\tau}\right) V_e(\rho). \tag{9}$$

As it is seen in Eq. (9), the relative change due to an incident is expressed in the pressure term. To see its connection with the changes in the equilibrium speed, let us equivalently write Eq. (9) as follows:

$$P^*(\rho) = V_{\max} - \left(1 + \frac{\alpha}{\tau}\right) V_e^*(\rho), \tag{10}$$

with α^* and $V_e^*(\rho)$ defined as:

$$\alpha^* = \alpha\beta + \beta\tau - \tau \tag{11}$$

$$V_e^*(\rho) = \beta V_e(\rho) \tag{12}$$

Both α and β can depend on space and time. The meaning of these parameters and the values they are allowed to take are detailed in Section 3.2. Note that if there is no incident, α^* is equal to zero which means that $\alpha = 0$ and $\beta = 1$.

Having all the ingredients, we are now ready to define the suggested incident traffic flow (ITF) model used to describe the traffic behaviour in the presence of an incident.

Definition 1. Incident traffic flow (ITF) model is defined as follows:

$$\rho_t + (\rho v)_x = 0, \tag{13}$$

$$v_t + \left(v - \rho \frac{dP^*(\rho)}{d\rho}\right) v_x = \frac{1}{\tau}\left(V_e^*(\rho) - v\right), \tag{14}$$

where

$$P^*(\rho) = P(\rho) - \frac{\alpha^*}{\tau} V_e(\rho). \tag{15}$$

Comparing Eqs. (4) and (14), which are respectively the momentum equation of the incident free (nominal ARZ) model and that of the ITF model, makes it clear that in the latter, the incident has been characterised by modifying the relaxation and traffic pressure terms. It is interesting to observe that we can see this connection better by rewriting the momentum equation of the ITF model in the form of Eq. (5). To see this, consider the momentum equation of the ITF model Eq. (14). Using Eqs. (10) and (12) we have:

$$v_t + v v_x + \frac{\mathrm{d}V_e^*}{\mathrm{d}\rho}\rho v_x + \frac{\alpha}{\tau}\frac{\mathrm{d}\left(V_e^*(\rho)\right)}{\mathrm{d}\rho}\rho v_x = \frac{1}{\tau}\left(V_e^*(\rho) - v\right). \tag{16}$$

Equivalently, we can write:

$$\begin{aligned} v_t + v v_x + \frac{\mathrm{d}V_e^*}{\mathrm{d}\rho}\rho v_x & \\ &= \frac{1}{\tau}\left(V_e^*(\rho) - \frac{\mathrm{d}\left(V_e^*(\rho)\right)}{\mathrm{d}\rho}\alpha\rho v_x - v\right) \\ &\cong \frac{1}{\tau}\left(V_e^*(\rho - \alpha\rho v_x) - v\right) \\ &= \frac{1}{\tau}\left(V_e^*(\rho + \alpha\rho_t + \alpha v\rho_x) - v\right) \\ &= \frac{1}{\tau}\left(V_e^*(\rho + \alpha D_t(\rho)) - v\right) \\ &= \frac{1}{\tau}\left(V_e^*(\rho^*) - v\right), \end{aligned} \tag{17}$$

where $D_t(.)$ stands for the material derivative. Note that the third line in Eq. (17) is derived by means of Taylor expansion, while the forth one is through the vehicle conservation law in Eq. (1). Having the momentum equation of the ITF model in the form of Eq. (17), it is easier to make the comparison with the momentum equation of the nominal ARZ model formed in Eq. (5). The main difference between Eqs. (17) and (5) is in the equilibrium speed, i.e., with the presence of an incident, drivers relax their speed based on a modified equilibrium speed V_e^* rather than V_e. Moreover, inspired by De Angelis (1999), in the presence of an incident,

drivers may feel the fictitious density $\rho^* = \rho + \alpha D_t(\rho)$ rather than the actual density ρ in the upstream of the incident. Note that the parameter α in ρ^*, represents a scaling factor for density variation. The larger the value of α, the larger the difference between ρ and ρ^*. Accordingly, there is a more severe abnormal traffic condition expected by the driver.

3. Mathematical properties of the ITF model

As it is perceived in Eq. (8), the pressure term makes a direct effect on the eigenvalues of the matrix $A(.)$ (the Jacobian of the flux in Eq. (7)) and consequently on the structural properties of the ITF model. In this section, we first investigate whether the modification in the pressure term makes any change in the characteristical properties of the ITF model compare to the nominal ARZ model. More specifically, we answer the question that whether the ITF model respects the anisotropy property of the traffic flow. Furthermore, in this section, we also discuss on the accepted bounds that the incident parameters α^*, α, and β in the ITF model can take.

3.1. ITF model: basic characteristics

To inspect the characteristics of the proposed ITF model, let us consider Eqs. ((13) and (14) without the relaxation term. We can write this set of equations in the form of Eq. (7) with $A(U)$ defined as

$$A(U) = \begin{bmatrix} v & \rho \\ 0 & v - \rho P^*_\rho(\rho) \end{bmatrix}. \tag{18}$$

Hence, the eigenvalues and the corresponding eigenvectors of the system can be obtained as

$$\lambda_1 = v - \rho P^*_\rho(\rho) \leq \lambda_2 = v, \tag{19}$$

$$r_1 = \begin{bmatrix} 1 \\ 0 \end{bmatrix}, r_2 = \begin{bmatrix} 1 \\ -P^*_\rho(\rho) \end{bmatrix}. \tag{20}$$

Equations (19) and (20) can give us information about the waves associated to these eigenvalues and also the mathematical properties of Eq. (18) Mammar et al. (2009). From Eqs. (19) and (20), we can infer that λ_2 is linearly degenerate and therefore the waves corresponding to this eigenvalue are contact discontinuities, i.e., waves separating two states with similar speeds but different densities. Assuming the convexity of the function $\rho P^*_\rho(\rho)$, Aw and Rascle (2000), the first eigenvalue is genuinely nonlinear and the associated waves are either rarefaction (corresponding to acceleration) or shock waves (corresponding to braking). Consequently, in the ITF model, all waves propagate at the speed at most equal to the velocity of the corresponding state; the anisotropy principle is preserved.

3.2. Incident parameters

As it is stated in Definition (1), in the ITF model, the effect of an incident is captured by the parameter α^* that is structured by α and β. While the first term gives a degree of freedom to introduce an incident-related anticipation time for drivers experiencing the abnormal situation, the latter describes the difference in the equilibrium speed to which drivers relax their speed. Obviously, α and β have positive values since they are respectively associated with the anticipation time and multiplication factor in the equilibrium speed. In addition, based on the meaning of the equilibrium speed $V^*_e(\rho)$, β should be bounded as follows:

$$0 \leq \beta \leq 1. \tag{21}$$

On the other hand, due to the relaxation term in Eq. (14), the so called sub-characteristic condition needs to be satisfied. Based on Rascle (2002), to meet the sub-characteristic condition the following inequality needs to be satisfied:

$$-\frac{dP^*}{d\rho} \leq \frac{dV^*_e(\rho)}{d\rho}, \tag{22}$$

Assuming $V^*_e(\rho)$ is a decreasing function of ρ, from the above equation, the following bound for the parameter α can be derived:

$$\alpha \geq 0. \tag{23}$$

In addition, since the traffic pressure term is an offset of the mean speed from the maximum speed, it is expected that incident makes this offset larger. As a result, the larger values of pressure induce the following condition:

$$P^*(\rho) = P(\rho) - \frac{\alpha^*}{\tau} V_e(\rho) \geq P(\rho), \tag{24}$$

which results in:

$$\alpha^* \leq 0. \tag{25}$$

The previous definition of incident parameters give rise to range incidents from incident-free to complete lane blockage as formulated in the next Proposition.

Proposition 1. ConsideringEq. (10), $\beta = 0$ results in maximum pressure value, i.e., $P^*(\rho) = V_{\max}$. In this case, the speed offset reaches its maximum and the speed dynamics asymptotically converges to zero, i.e., it corresponds to full lane closure.

The proof can be found in Appendix B. This situation presented in Proposition 1 corresponds to the complete lane closure resulting in the convergence of the speed profile to zero.

4. Discretisation of the ITF model

As it is seen in Definition (1), due to the presence of the relaxation term, the PDEs describing the ITF model is non-homogeneous. Hence, to discretise the model, we have applied the two steps splitting method Toro (1999). In the first step, the homogenous system is discretised by the conventional use of the Godunov method. The second step is then followed by solving an ODE with its initial condition obtained from the first step. To be more precise, consider a non-homogeneous PDE with an initial value as follows:

$$\begin{cases} U_t + F_x(U) = G(U), \\ U(x, t^n) = U^n \ : \ \text{initial condition} \end{cases} \tag{26}$$

In order to find the solution U^{n+1} from the initial value U^n, splitting method suggests to separate the source term from the original PDE and start with the following homogeneous PDE:

$$\begin{cases} U_t + F_x(U) = 0, \\ U(x, t^n) = U^n \ : \ \text{initial condition} \end{cases} \Rightarrow \overline{U}^{n+1} \tag{27}$$

Afterward, the solution of the above step is used as an initial condition for solving the following ODE:

$$\begin{cases} \frac{d}{dt} U = G(U), \\ \overline{U}^{n+1} \ : \ \text{initial condition} \end{cases} \Rightarrow U^{n+1} \tag{28}$$

4.1. Conservation form of the ITF model

Before applying the splitting method for discretising the ITF, we first need to rewrite the ITF model in the conservation form of Eq. (26). Let us first consider the homogeneous ITF model in the following form:

$$\rho_t + (\rho v)_x = 0, \tag{29}$$

$$(v+P^*(\rho))_t + v(v+P^*(\rho))_x = 0 \quad . \tag{30}$$

In order to write the model as a conservation law of the form:

$$U_t + F_x(U) = 0, \tag{31}$$

it is enough to multiply the Eq. (29) by $v + P^*(\rho)$ and Eq. (30) by ρ. By summing them up, the desirable structure can be obtained as

$$\begin{aligned} &\rho_t + (\rho v)_x = 0, \\ &(\rho(v+P^*(\rho)))_t + (\rho v(v+P^*(\rho)))_x = 0, \end{aligned} \tag{32}$$

where $P^*(\rho)$ is defined as inEq. (9). Consequently,

$$U = \begin{bmatrix} \rho \\ \rho\left(v - \left(1+\frac{\alpha^*}{\tau}\right)V_e(\rho)\right) \end{bmatrix} = \begin{bmatrix} \rho \\ m \end{bmatrix}, \tag{33}$$

and $F(U)$ in Eq. (31) can be formed as

$$F(U) = \begin{bmatrix} m + \rho\left(1+\frac{\alpha^*}{\tau}\right)V_e(\rho) \\ \frac{m^2}{\rho} + m\left(1+\frac{\alpha^*}{\tau}\right)V_e(\rho) \end{bmatrix}, \tag{34}$$

or equivalently as

$$F(U) = \begin{bmatrix} q \\ q\left(v - \left(1+\frac{\alpha^*}{\tau}\right)V_e(\rho)\right) \end{bmatrix} = \begin{bmatrix} q \\ z \end{bmatrix}, \tag{35}$$

with $q = \rho v$ which is the traffic flow. If the relaxation term is also considered in the ITF model, the right hand side of the Eq. (31) is a nonzero term and resulted from simple reordering as

$$G(U) = \begin{bmatrix} 0 \\ -\frac{m}{\tau} - \frac{\sigma\rho}{\tau^2}V_e(\rho) \end{bmatrix}, \tag{36}$$

where

$$\sigma = \alpha^* + \tau - \beta\tau = \alpha\beta. \tag{37}$$

Now we can start with the discretisation following the two steps of the splitting method.

4.2. First step: Godunov discretisation of the homogeneous PDE

Consider Eq. (27) where $F(U)$ is the flux matrix. The Godunov scheme is based on gridding the time and space domain in order to generate cells and updating U^n in each cells for the next time step $n+1$. Godunov discretisation is based on the conservation law briefed in Appendix B. We refer the interested readers to Toro (1999) and Mammar et al. (2009) for more details of the Godunov discretisation.

Defining the conservation form of the ITF model in (32) and considering Eqs. (33)–(35), a Riemann problem should be solved in each boundary point to get $F_{i\pm1/2}$ introduced in (50). As a result, with the initial state of $[\rho_i^n, m_i^n]^T$, the following update equations are obtained Mammar et al. (2009):

$$\begin{aligned} \overline{\rho}_i^{n+1} &= \rho_i^n + \frac{\Delta t}{\Delta x}\left(q_{i-1}^n - q_i^n\right) \\ \overline{m}_i^{n+1} &= m_i^n + \frac{\Delta t}{\Delta x}\left(z_{i-1}^n - z_i^n\right). \end{aligned} \tag{38}$$

4.3. Second step: ODE discretisation

Recalling $G(U)$ defined in Eq. (36), the ODE formed in Eq. (28) can be expanded as

$$\begin{cases} \dfrac{d\rho}{dt} = 0 \\ \dfrac{dm}{dt} = -\dfrac{m}{\tau} - \dfrac{\sigma\rho}{\tau^2}V_e(\rho) \\ \text{Initial data: } \left[\overline{\rho}^{n+1}, \overline{m}^{n+1}\right]^T. \end{cases} \tag{39}$$

Hence, the final move is to solve Eq. (39) by applying the trapezoidal method to get the following update of ρ and m:

$$\begin{aligned} \rho_i^{n+1} &= \overline{\rho}_i^{n+1}, \\ m_i^{n+1} &= a_f \overline{m}_i^{n+1} - \frac{2\sigma_i \Delta t \overline{\rho}_i^{n+1}}{\tau(2\tau+\Delta t)}V_e\left(\overline{\rho}_i^{n+1}\right), \end{aligned} \tag{40}$$

with a_f defined as below:

$$a_f = \left(\frac{1-\frac{\Delta t}{2\tau}}{1+\frac{\Delta t}{2\tau}}\right). \tag{41}$$

5. Incident parameter estimation

In this section, we aim at developing an algorithm in order to estimate the incident parameters α_i and β_i. These parameters correspond to the effect that incident may cause in the segment i. Note that recalling Eqs. (35)–(37), α_i and β_i are reflected in the discretised ITF model through the parameters α_i^* and σ_i. Clearly seen from Eqs. (11) and (37), there is a one to one relation between these two set of parameters. Moreover, the bounds on α and β for segment i found in Eqs. (21) and (23) can be transformed in terms of α_i^* and σ_i as

$$0 \le \frac{\alpha_i^* - \sigma_i + \tau}{\tau} \le 1, \tag{42}$$

$$\frac{\sigma_i \tau}{\alpha_i^* - \sigma_i + \tau} \ge 0 \tag{43}$$

As it is emphasized in Section 4, at each time step n and for each segment i, two Riemann problems need to be solved in order to calculate $F(U_{i-1/2}(0))$ as well as $F(U_{i+1/2}(0))$. The estimation algorithm used is an on-line, constrained nonlinear receding horizon algorithm Rao (2000). At each time step n, an optimization problem with a specific cost function is solved to obtain the estimate of α_i^{*n} and σ_i^n denoted by $\hat{\alpha}_i^{*n}$ and $\hat{\sigma}_i^n$. These estimated parameters are then used for solving the Riemann problem in the ITF model in order to generate U^{n+1}. The selected objective function at time step n introduced as

$$J_n = \left(\rho_i^n - \hat{\rho}_i^n\right)^2 + \eta\left(v_i^n - \hat{v}_i^n\right)^2 + \gamma\left(\hat{\alpha}_i^{*n} - \hat{\alpha}_i^{n-1}\right)^2 + \zeta\left(\hat{\sigma}_i^n - \hat{\sigma}_i^{n-1}\right)^2. \tag{44}$$

The parameters η, γ and ζ are constant and pre-selected weighting parameters and $i+1$ is the segment that incident has been occurred in it. $\hat{\rho}$ and $\hat{v}$ are the measured density and speed respectively. Consequently, the optimization problem can be formulated as

$$\min_{\alpha_i^*, \sigma_i} \quad J_n \tag{45}$$

$$\text{subjected to} \quad (38),\ (40),\ (42),(43)$$

6. Case study

The capability of the proposed ITF model to reproduce the traffic dynamics under incident condition is investigated in a hypothetical freeway with 7 segments. The schematic representation of this hypothetical freeway is depicted in Fig. 2. As it is seen from Fig. 2, each

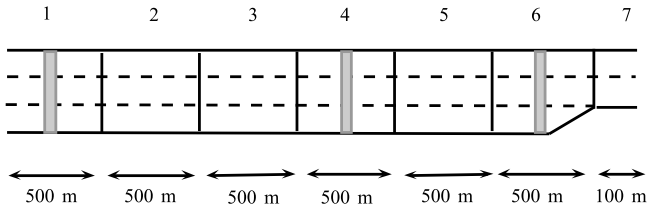

Fig. 2. Hypothetical freeway in the case study.

Table 1
Nominal parameter identification result.

ρ_{max} (veh/km)	480
V_{max} (km/h)	125.2741
ρ_{cr} (veh/km)	62.2147
V_{cr} (km/h)	104.7662
τ (s)	5.4653
W_{max}	23.3915

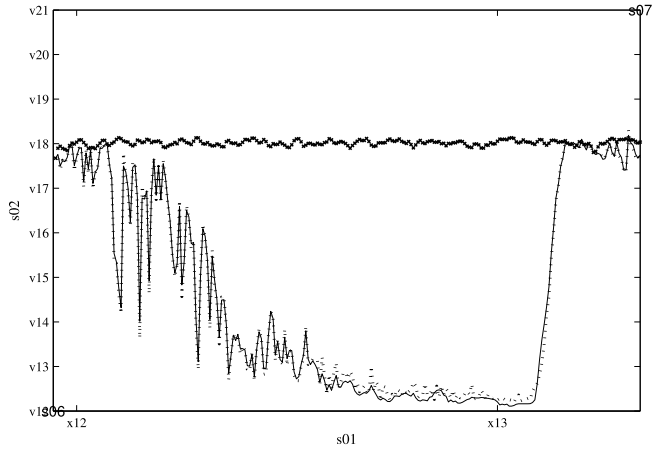

Fig. 3. Speed variation in the forth segment. Dashed line is the simulation data, solid line is the ITF model with estimated $\hat{\alpha}^*$. Stars are the simulation result

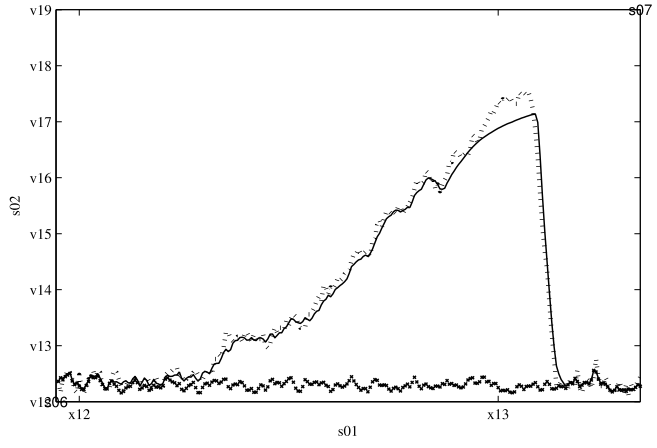

Fig. 4. Density in the forth segment. Dashed line is the simulation data, solid line is the ITF model with estimated $\hat{\alpha}^*$ and star line is the simulation result with

segment, except for the last one, has three lanes and length of 500 m. The last segment has two lanes with the length of 100 m. The freeway is

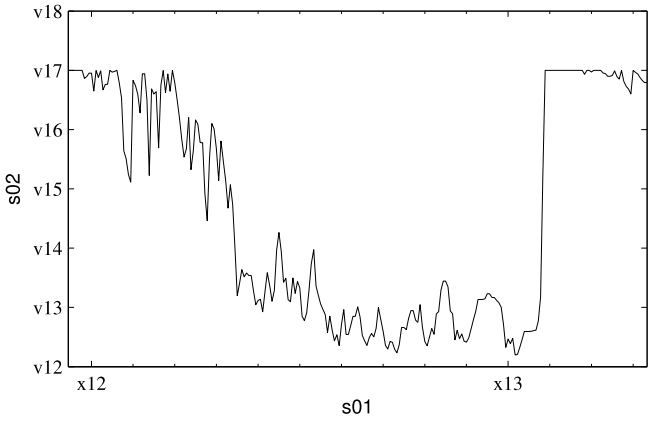

Fig. 5. Estimated $\hat{\alpha}^*$ in the forth segment.

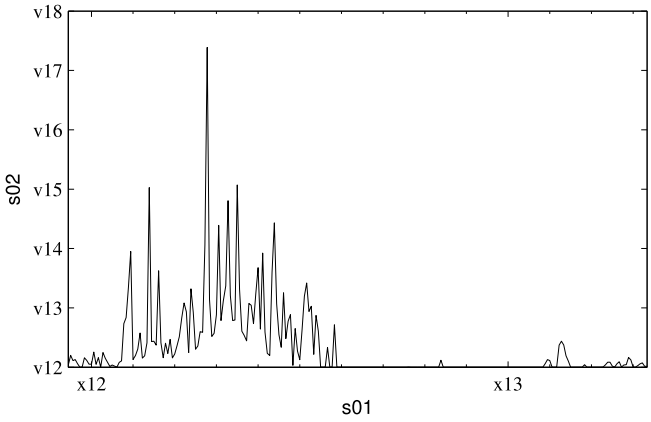

Fig. 6. Estimated incident related anticipation time $\hat{\alpha}$ in the forth segment.

assumed to be equipped with sensors which are indicated by a grey box in the Figure.

Two datasets of 3 h each, were generated by simulation. The first part of the simulation scenario (up to time $t = 1.5$ h) has been used to offline identify all of the nominal model parameters excluding the incident parameters (α^* and σ are kept zero in this phase). This result are shown in Table 1. The simulation setup has been chosen in a way that after $t = 1.5$ h, an incident happens in the beginning of the fifth segment and lasts for half an hour. During this period, drivers are not allowed to use two out of three lanes in the fifth segment. This part of simulation scenario has been used for online estimation of α^* and σ.

The speed and density of in the fourth segment form the simulation data, the suggested ITF model and the nominal ARZ model are shown in Figs. 3 and 4 respectively. As it is expected, due to the incident in segment 5, there is a sudden change in the speed and density variation of the upstream segment. Congestion started after 10 min and the segment becomes fully congested before the incident is resolved at $t = 2$ h. The density then starts to decrease with sharp slope because vehicles are suddenly allowed to use all the three lanes of the fifth segment. As it is illustrated in Figs. 3 and 4, the ITF model with the estimated incident parameters is capable to model the incident's effect. Without including the estimated incident parameter information, the nominal ARZ model is not successful in properly capture the traffic dynamics in the presence of an incident.

Values of $\hat{\alpha^*}$ are plotted in Fig. 5. At the time when the incident starts, $\hat{\alpha^*}$ diverge from zero and takes nonzero values. The parameter goes back to zero with some overshoot after the incident is dissolved.

The parameters α and β can be reconstructed from the estimated

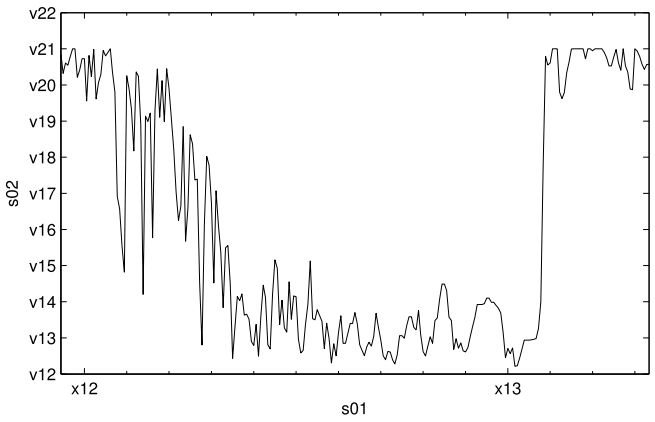

Fig. 7. Estimated scaling factor $\hat{\beta}$ as a function of time.

parameters of α^* and σ using Eqs. (11) and (37). In Fig. 6, the reconstructed $\hat{\alpha}$ which represents the incident related anticipation time is depicted. From Fig. 6, $\hat{\alpha}$ takes positive values for 15 min after the incident. This is the time when the density increased to almost 120 (veh/km), being twice as high as the critical density. After this interval, $\hat{\alpha}$ becomes zero until the incident is dissolved. Zero value of $\hat{\alpha}$ indicates the equivalence between density ρ and fictitious density ρ^*. In other words, since the road is already fully congested, the density which drivers think they might experience in the future is the same as the current density.

Parameter $\hat{\beta}$ which is the scaling factor of the equilibrium speed is plotted in Fig. 7 as a function of time. As it is expected, $\hat{\beta}$ is 1 before the incident and decreases to almost 0.2 in the incident interval. After the incident, value of $\hat{\beta}$ returns to 1.

7. Conclusions

In this paper, an incident traffic flow (ITF) model has been proposed to reproduce the traffic dynamics under incident. Within the context of second order macroscopic flow models, traffic pressure term is augmented by appropriately structured incident parameters. A multi step discretisation method is then proposed to approximate the solution of the PDE by ODEs. Furthermore, the proposed ITF model has been analysed. To show the importance of incident parameter inclusion, an online estimation method is used in order to recover the effect of incidents.

Further research attention focuses on validation of the model with real data. Moreover developing incident tolerant traffic management solutions on the basis of the ITF model as well as connect ITF to learning algorithms are among future related research directions.

Declaration of competing interest

The authors declare that they have no known competing financial interests or personal relationships that could have appeared to influence the work reported in this paper.

Acknowledgements

This work has partially been supported and funded by the Transport Area of Advance. The project IRIS is acknowledged for financial support.

Electronic Supplementary Material

Supplementary data to this article can be found online at https://doi.org/10.1016/j.commtr.2022.100060.

Appendix

A

Assume a uniform girding on the domain $[x_L, x_R]$ to get N subsegments with discrete points at

$$x_i = x_L + \left(i + \frac{1}{2}\right)\Delta x \quad \text{for} \quad i = 0, 1, \ldots, N \tag{47}$$

and boundaries can be regarded as

$$x_{i-1/2} = x_i - \frac{\Delta x}{2} = x_L + i\Delta x \quad \text{for} \quad i = 0, 1, \ldots, N+1 \tag{48}$$

If U_i^n be regarded as the state in segment i at time step n, Godunov scheme emphasized that the state, which is the conserved variables, is updated for the next time step by the following conservation equation:

$$U_i^{n+1} = U_i^n + \frac{\Delta t}{\Delta x}\left[F_{i-1/2} - F_{i+1/2}\right], \tag{49}$$

where the intercell fluxes $F_{i-1/2}$ and $F_{i+1/2}$ are obtained as

$$\begin{cases} F_{i-1/2} = F\left(U_{i-1/2}(0)\right) \\ F_{i+1/2} = F\left(U_{i+1/2}(0)\right), \end{cases} \tag{50}$$

and $U_{i+1/2}(0)$ refers to the exact solution $U_{i+1/2}(x/t)$ of the Riemann problem $RP(U_i^n, U_{i+1}^n)$ evaluated at $x/t = 0$; the solution is evaluated along the intercell boundary, which coincide with the t-axis in the local frame of the Riemann solution.

B

Proof 1 In case of $\beta = 0$, the pressure term $P^*(\rho) = V_{\max}$. Consequently from Eqs. (14) and (12), the momentum equation of the ITF model takes the following form:

$$v_t + vv_x = -\frac{v}{\tau}. \tag{51}$$

Since $v(x(t), t) = \frac{dx(t)}{dt}$, the solution to the Eq. (51) can be obtained as

$$\begin{cases} \dfrac{dx(t)}{dt} = v(x(t), t) \\ \dfrac{dv(x(t), t)}{dt} = -\dfrac{v(x(t), t)}{\tau}, \end{cases} \tag{52}$$

Introduce $z(t) = v(x(t), t)$, then:

$$\begin{cases} \dfrac{dx(t)}{dt} = z(t) \\ \dfrac{dz(t)}{dt} = -\dfrac{z(t)}{\tau}, \end{cases} \tag{53}$$

which is a system of coupled ODE in the form of:

$$\frac{dX(t)}{dt} = AX(t), \tag{54}$$

where

$$X(t) = \begin{bmatrix} x(t) \\ z(t) \end{bmatrix}, \tag{55}$$

and

$$A = \begin{bmatrix} 0 & 1 \\ 0 & -\dfrac{1}{\tau} \end{bmatrix}. \tag{56}$$

The generic solution to Eq. (54) can be written as

$$X(t) = C_1 h_1 e^{\mu_1 t} + C_2 h_2 e^{\mu_2 t}, \tag{57}$$

with C_1 and C_2 as some constants. Since with finite $\tau > 0$, the eigenvalues of A become $\mu_1 = 0$ and $\mu_2 = -\frac{1}{\tau}$, we can select the corresponding eigenvectors as $h_1 = \begin{bmatrix} 1 \\ 0 \end{bmatrix}$ and $h_2 = \begin{bmatrix} -\tau \\ 1 \end{bmatrix}$. Therefore, we obtain the solution as

$$\begin{cases} x(t) = C_1 - \tau C_2 e^{\frac{-t}{\tau}} \\ z(t) = C_2 e^{\frac{-t}{\tau}}, \end{cases} \tag{58}$$

where C_1 and C_2 depend on the initial values of $x(t)$ and $z(t)$. Equation (58) implies that $z(t)$ asymptotically goes to zero by evolving in time, i.e., complete lane closure.

References

Aw, A., Rascle, M., 2000. Resurrection of second order models of traffic flow. SIAM J. Appl. Math. 60, 916–938.

Cremer, M., Papageorgiou, M., 1981. Parameter identification for a traffic flow model. Automatica 17, 837–843.

Dabiri, A., Kulcsár, B., 2015. Freeway traffic incident reconstruction - a bi-parameter approach. Transport. Res. C Emerg. Technol. 58, 585–597.

Dabiri, A., Kulcsár, B., 2017. Distributed ramp metering-a constrained discharge flow maximisation approach. IEEE Trans. Intell. Transport. Syst. 1–14.

Dabiri, A., Kulcsár, B., Köroğlu, H., 2017. Distributed LPV state-feedback control under control input saturation. IEEE Trans. Automat. Control 62, 2450–2456.

Daganzo, C.F., 1995. Requiem for second-order fluid approximation of traffic flow. Transport. Res. Part B 29, 227–286.

De Angelis, E., 1999. Nonlinear hydrodynamic models of traffic flow modeling and mathematical problems. Math. Comput. Model. 29, 83–95.

Hajiahmadi, M., van de Weg, G.S., Tampére, C.M.J., Corthout, R., Hegyi, A., De Schutter, B., Hellendoorn, H., 2016. Integrated predictive control of freeway networks using the extended link transmission model. IEEE Trans. Intell. Transport. Syst. 17, 65–78.

Hegyi, A., De Schutter, B., Hellendoorn, H., 2005a. Model predictive control for optimal coordination of ramp metering and variable speed limits. Transport. Res. C Emerg. Technol. 13, 185–209.

Hegyi, A., De Schutter, B., Hellendoorn, J., 2005b. Optimal coordination of variable speed limits to suppress shock waves. IEEE Trans. Intell. Transport. Syst. 6, 101–112.

Hegyi, A., Girimonte, D., Babuska, R., De Schutter, B., 2006. A comparison of filter configurations for freeway traffic state estimation. In: IEEE Conference on Intelligent Transportation Systems, pp. 1029–1034.

Knoop, V., 2009. Road Incidents and Network Dynamics Effects on Driving Behaviour and Traffic Congestion. TRAIL Research School. Ph.D. thesis. TRAIL Thesis Series T2009/13.

Knoop, V., Zuylen, H., Hoogendoorn, S., 2009. Microscopic Traffic Behaviour Near Incidents. Transportation and Traffic Theory: Golden Jubilee. Springer, US, pp. 837–843.
Luspay, T., Kulcsár, B., van Wingerden, J.W., Verhaegen, M., Bokor, J., 2011. Linear parameter varying identification of freeway traffic model. IEEE Transact. Control Syst. Technol. 19, 31–45.
Mammar, S., Lebacque, J.P., Salem, H.H., 2009. Riemann problem resolution and godunov scheme for the Aw-Rascle-Zhang model. Transport. Sci. 43, 531–545.
Rao, C.V., 2000. Moving Horizon Strategies for the Constrained Monitoring and Control of Nonlinear Discrete-Time Systems. Ph.D. thesis. Univ. Wisconsin-Madison.
Rascle, M., 2002. An improved macroscopic model of traffic flow: derivation and links with the lighthill-whitham model. Math. Comput. Model. 35, 581–590.
Sanwal, K.K., Petty, K., Walrand, J., Fawaz, Y., 1996. An extended macroscopic model for traffic flow. Transport. Res. Part B 30, 1–9.
Toro, E.F., 1999. Riemann Solvers and Numerical Methods for Fluid Dynamics: A Practical Introduction. Springer.
Wang, Y., Papageorgiou, M., Messmer, A., Coppola, P., Tzimitsi, A., Nuzzol, A., 2009. An adaptive freeway traffic state estimator. Automatica 45, 10–24.
Zhang, H., 2002. A non-equilibrium traffic model devoid of gas-like behavior. Transport. Res. Part B 36, 275–290.

Azita Dabiri received the Ph.D. degree from the Automatic Control Group, Chalmers University of Technology, in 2016. She was a Post-Doctoral Researcher with the Department of Transport and Planning, TU Delft, from 2017 to 2019. In 2019, she received an ERCIM Fellowship and also a Marie Curie Individual Fellowship which allowed her to perform research at the Norwegian University of Technology (NTNU) as a Post-Doctoral Researcher from 2019 to 2020, before joining the Delft Center for Systems and Control, TU Delft, as an Assistant Professor. Her research interests are in the area of integration of model-based and learning-based control and its applications in transportation networks.

Balázs Kulcsár received the M.Sc. degree in traffic engineering and the Ph.D. degree from Budapest University of Technology and Economics (BUTE), Budapest, Hungary, in 1999 and 2006, respectively. He has been a Researcher/Post-Doctor with the Department of Control for Transportation and Vehicle Systems, BUTE, the Department of Aerospace Engineering and Mechanics, University of Minnesota, Minneapolis, MN, USA, and with the Delft Center for Systems and Control, Delft University of Technology, Delft, The Netherlands. He is currently a Professor with the Department of Electrical Engineering, Chalmers University of Technology, Göteborg, Sweden. His main research interest focuses on traffic flow modeling and control.